

Synthesis and Characterization of Nano-Structured α -MnO₂/Co₃O₄ Metal Oxide for Energy Storage Application

M.Sc. Thesis

By

MANOJ KUMAR



DISCIPLINE OF PHYSICS

INDIAN INSTITUTE OF TECHNOLOGY INDORE

JUNE 2019

Synthesis and Characterization of Nano-Structured α -MnO₂/Co₃O₄ Metal Oxide for Energy Storage Application

A THESIS

*Submitted in partial fulfilment of the
requirements for the award of the degree*

of

Master of Science

By

MANOJ KUMAR



DISCIPLINE OF PHYSICS

INDIAN INSTITUTE OF TECHNOLOGY INDORE

JUNE 2019



INDIAN INSTITUTE OF TECHNOLOGY INDORE

CANDIDATE'S DECLARATION

I hereby certify that the work which is being presented in the thesis entitled **Synthesis and Characterization of Nano-Structured α -MnO₂/Co₃O₄ Metal Oxide for Energy Storage Application** in the partial fulfilment of the requirements for the award of the degree of **MASTER OF SCIENCE** and submitted in the **DISCIPLINE OF PHYSICS, Indian Institute of Technology Indore**, is an authentic record of my own work carried out during the time period from July 2017 to June 2019 under the supervision of **Dr. Parasharam M. Shirage**, Associate Professor, IIT Indore. The matter presented in this thesis has not been submitted by me for the award of any other degree of this or any other institute.

Manoj Kumar.

Signature of the student with date
(Manoj Kumar)

This is to certify that the above statement made by the candidate is correct to the best of my knowledge.

Signature of the Supervisor of M.Sc. thesis
(Dr. Parasharam M. Shirage)

Dr. Parasharam M. Shirage
28/6/2019

Manoj Kumar has successfully given his M.Sc. Oral Examination held on **20 June 2019**

Dr. Parasharam M. Shirage
28/6/2019
Signature of Supervisor of MSc thesis
Date:

Dr. Preeti Anand Bhoje
Signature, DPGC
Date: 1/7/19

Signature of PSPC Member
Date: 1/7/19

Preeti
Dr. Preeti Anand Bhoje

Signature of PSPC Member
Date: 28/6/19

Dr. Abhijeet Joshi
Dr. Abhijeet Joshi

Dedicated with much love and affection

to:-

my beloved country,

my Teachers,

my Guide,

and my family.

Acknowledgements

It is always an immense pleasure to remind the fine people for their sincere support and encouragement I received to uphold my project work. This work will not have been completed without their kind help.

I take this opportunity to express my deep sense of thank and profound gratitude to my supervisor, **Dr. Parasharam M. Shirage** for giving me opportunity to work in AFMRG. His exemplary guidance, monitoring and constant encouragement helped me in successful completion of this work well on time. I am thankful to my PSPC members **Dr. Preeti Anand Bhoje** and **Dr. Abhijeet Joshi**, for their valuable suggestions which helped me to enhance my experimental skills.

I am deeply indebted to **Prof. Pradeep Mathur** (Director, Indian Institute of Technology, Indore) for allowing me to carry out my research in this institution. I greatly appreciate the support and motivation of all physics department of IIT Indore.

I am heartily thankful to **L. Sinha** and Rahul Lamba for their kind support and help to accomplish my project successfully. I extend my thanks to complete AFMRG lab for their kind help throughout the project work. I am highly thankful to SIC, IIT Indore for FESEM and XRD measurements as without their support this report would not have been possible.

I am in short of words in expressing my heartfelt gratitude to my family who paved the path before me upon whose shoulders I stand. To my parents and sisters for their continuous support, encouragement and motivation in every phase of life, I won't be this strong without you all as my inspiration.

Manoj Kumar

Abstract

A **capacitor** is a passive terminal electrical device that is used to store electrostatic energy in the form of electric field separated by a dielectric, but as a drawback, this device is not able to hold a large energy that is our primary focus and concern in response to the changing global high energy demand and needs in the future. Looking into the concern of future global energy crisis, a device that can solve our energy storage related problem is the **supercapacitor** which has matured significantly over the last decade and emerged with the potential to facilitate major advances in energy storage. More importantly, a supercapacitor has a large capacitance (in farad) which is approx. thousands times larger than a simple electrolytic capacitor and can full fill our future energy storage requirement due to having high power density, fast charging and discharging, and long service life as compared to batteries. Not only this, supercapacitors have many applications such as they are widely used in renewable energy power plant, memory back-up devices and hybrid electrical vehicles etc.

Here we report the synthesis and supercapacitive property of Manganese dioxide (α -MnO₂) and its hybrid with Cobalt oxide (Co₃O₄) nanostructure synthesized by hydrothermal method. We also performed several characterizations such as; X-ray diffraction (XRD), Field Emission Scanning Electron Microscopy (FESEM) and Brunauer Emmett Teller (BET), UV-Visible spectroscopy, Infrared spectroscopy to know about the purity, crystal structure, morphology and surface related information of the desired nanostructure.

The electrochemical characterization of α -MnO₂ resulted the capacitance of 570 F/g at the scan rate of 1mV/s whereas hybridized α -MnO₂/Co₃O₄ exhibited an enhanced capacitance of 1802 F/g. The material shows an excellent stability and capacitive retention of 96.5% after 2000 cycles. Hence these electrochemical results of α -MnO₂ and Co₃O₄ hybrid nanostructured demonstrate its application for energy storage devices.

Table of Contents

List of Figures	vii
List of Tables	ix
Acronyms	X
Chapter 1: Introduction	1
1.1 Importance of nanotechnology in the field of supercapacitors.....	7
1.2 Hydrothermal synthesis	8
1.3 Transition metal oxide based electrodes.....	9
Chapter 2: Material Synthesis & Characterization Techniques	11
2.1 Synthesis of α -MnO ₂ Material.....	11
2.2 Synthesis of α -MnO ₂ /Co ₃ O ₄ Material.....	11
2.3 Characterization Techniques	12
• 2.3.1 X-ray diffraction	12
• 2.3.2 FE-SEM	15
• 2.3.3 TEM.....	18
• 2.3.4 BET (Brunauer, Emmett and Teller).....	19
• 2.3.5 UV-Visible Spectroscopy.....	20
2.4 Cyclic Voltammetry	21
2.5 Electrochemical Impedance Spectroscopy	23
2.6 Galvanostatic Charging Discharging	24

Chapter 3: Results & Discussion25

3.0 Physical Characterizations.....25

Part-A (Characterizations of α -MnO₂ and Analysis)

- A.1 XRD Analysis25
- A.2 FE-SEM Analysis27
- A.3 TEM Analysis.....27
- A.4 UV-Visible Analysis.....28
- A.5 BET Analysis29
- A.6 Electrochemical Analysis29
 - (a) A.6.1 CV Analysis.....30
- A.7 EIS Analysis.....31
- A.8 GCD Analysis32
- A.9 Stability Analysis33

Part-B (Characterization of α -MnO₂/Co₃O₄ and Analysis)

- B.1 XRD Analysis.....34
- B.2 UV-Visible Analysis.....34
- B.3 FE-SEM Analysis.....36
- B.4 TEM Analysis.....36
- B.5 BET Analysis.....37
- B.6 Electrochemical analysis.....38
 - (a) B.6.1 CV Analysis.....38
- B.7 EIS Analysis.....39
- B.8 GCD Analysis.....40

Chapter 4: Summary and Conclusion and Future Scope

4.1 Summary and Conclusion and Future scope..... 43

References48

List of Figures

1. Fig.1.1 Working Principle of battery.....	2
2. Fig.1.2 Parallel Plate Capacitor.....	3
3. Fig.1.3 Ragone Plot.....	5
4. Fig.1.4 Schematic diagram of EDLC.....	6
5. Fig.1.5 Schematic diagram of pseudo capacitor.....	6
6. Fig.1.6 Hydrothermal Synthesis.....	8
7. Fig.2.1 Lab instrument used for synthesis	12
8. Fig.2.2 Diagram showing X-Ray Production.....	13
9. Fig.2.3 Bragg's Diffraction	14
10. Fig.2.4 XRD Machine in the lab	15
11. Fig.2.5 Schematic working diagram of FE-SEM	16
12. Fig.2.6 Electron beam and Sample interaction.....	17
13. Fig.2.7 FE-SEM instrument setup at SIC, IIT Indore.....	17
14. Fig.2.8 Schematic of TEM.....	18
15. Fig.2.9 BET Facility at IIT Indore.....	20
16. Fig.2.10 Schematic For UV-Visible Spectrometer.....	21
17. Fig.2.11 Possible Transition of Organic Molecule.....	21
18. Fig.2.12 Schematic View of 3-electrode System.....	22
19. Fig.2.13 Electrochemical measurement set-up.....	23
20. Fig.3.1 X.R.D pattern of α -MnO ₂ nanostructure	26
21. Fig.3.2 Geometrical structure of α -MnO ₂	26
22. Fig.3.3 FE-SEM images of α -MnO ₂ with scale bar.....	27
23. Fig.3.4 TEM images of α -MnO ₂ nanorods.....	28
24. Fig.3.5 Tauc Plot of α -MnO ₂	28
25. Fig.3.6 Nitrogen adsorption-desorption isotherm and pore size distribution curve of α -MnO ₂	29
26. Fig.3.7 CV curve of α -MnO ₂ at different scan rate.....	30
27. Fig.3.8 Variation of specific capacitance with scan Rate of α -MnO ₂	30
28. Fig.3.9 EIS spectroscopy of α -MnO ₂	31
29. Fig.3.10 Galvanostatic charging/discharging plot of	

α -MnO ₂	32
30. Fig.3.11 Variation of specific capacitance with current Densities α -MnO ₂	33
31. Fig.3.12 Stability curve of α -MnO ₂ nanostructure.....	33
32. Fig.3.13 XRD pattern of α -MnO ₂ and α -MnO ₂ /Co ₃ O ₄	34
33. Fig.3.14 Tauc plot of α -MnO ₂ /Co ₃ O ₄	35
34. Fig.3.15 FE-SEM Images of α -MnO ₂ /Co ₃ O ₄	36
35. Fig.3.16 TEM of α -MnO ₂ /Co ₃ O ₄ nanorods.....	36
36. Fig.3.17 Nitrogen adsorption-desorption isotherm and pore size distribution curve of α -MnO ₂ /Co ₃ O ₄	37
37. Fig.3.17 CV curve of α -MnO ₂ /Co ₃ O ₄ hybrid at different scan rate.....	38
38. Fig.3.18 Variation of specific capacitance with scan rate.....	39
39. Fig.3.19 EIS spectroscopy of α -MnO ₂ /Co ₃ O ₄	39
40. Fig.3.20 Galvanostatic charging/discharging α -MnO ₂ /Co ₃ O ₄ plot.....	40
41. Fig.3.21 Variation of specific capacitance with current Densities of α -MnO ₂ /Co ₃ O ₄	41

List of Table

Table 1.1 Approximate evaluations between supercapacitors, capacitors and batteries.....	4
--	---

Acronyms

Acronyms	Meaning
MnO ₂	Manganese Dioxide
EDLS's	Electric Double Layer Capacitor
α	Alfa
β	Beta
XRD.	X-Ray Diffraction
Cu	Copper
BSE	Back Scattered Electron
Ni.	Nickel
WE	Working Electrode
CE	Counter Electrode
RE	Reference Electrode
CV	Cyclic Voltammetry
DC	Direct current
AC	Alternating current
EIS	Electrochemical impedance Spectroscopy
GCD	Galvanostatic Charging/Discharging
FE-SEM	Field Emission Scanning Electron Microscopy
CNT's	Carbon Nanotubes

CHAPTER -1

Introduction

As we already know that demand for energy is increasing globally day by day that is resulting in a shortage of traditional energy resources (like; fossil fuels, coal, non-renewable source of energy). Therefore, energy is going to be the center of interest for the economic powers of the world and smart people as well. There are some reasons for the global energy crisis that mainly includes overpopulation and thus overconsumption, wars, market manipulation, and unexplored renewable energy options, etc. that leads us to march toward an energy crisis. This energy crisis is getting dangerous for the efficient distribution of energy resources to an economy. Also, our conventional energy resources are limited. Therefore energy savings and efficiency are highly promoted by authorities and governments. These governments and authorities are promoting sustainable and renewable energies as an alternative to the limited conventional energy resources. Thus, the possible alternates that we have today are nuclear energy, solar (photovoltaic or thermal), wind, water, etc. which needs intense research and development aspects. But many of these alternates cannot provide us continuous energy throughout the day. Therefore energy storage devices come into play which can store energy during peak hours and can be utilized during off hours. Energy storage is employed to reduce the rate of mismatch between energy supply and energy demand. Moreover, energy storage can also play the role of a significant stakeholder in energy conservation. A renewable energy generation plant combined with the corresponding energy storage system can act as a constant power generation plant and can play a significant role in energy conservation as well.

We have three different types of energy storage devices:-

(1). Batteries. (2). Capacitors. (3). Supercapacitors.

Batteries:

As we know, the battery is an electrical power source that stores a particular amount of energy in electrical form and turns already stored chemical energy storage to electrical energy through the various chemical reactions. Nowadays, batteries are one the most used and informal source of power supply to the various electronic appliances, and in industries as well. Cells or Batteries have three essential components (1). The cathode (2). Anode and (3) An Electrolyte.

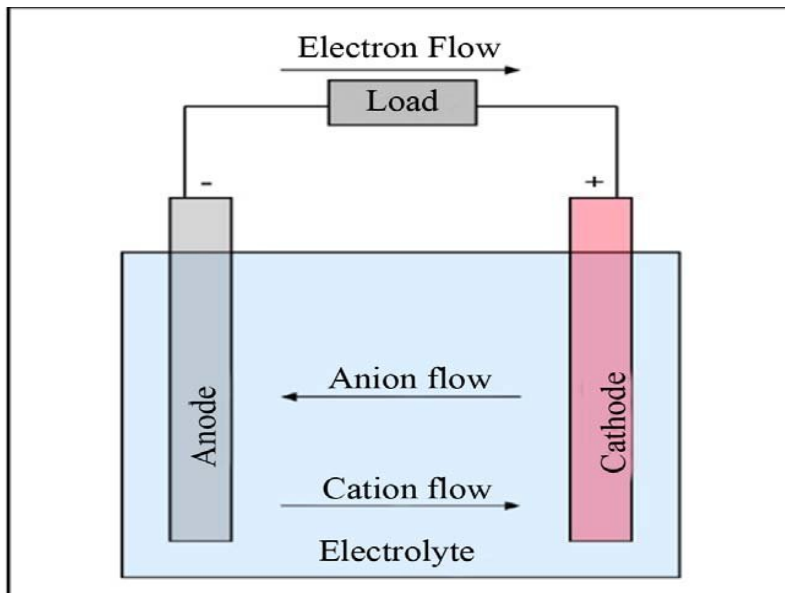


Fig. 1.1 Working principle of a battery [2]

When we connect two terminals of a battery to any external sources, then anions start their motion towards the anode, and similarly, cation starts moving towards the cathode and this movement will provide a current to the external device as shown in the above figure. This also results in the redox reaction, which is the basic phenomenon of working batteries. After a few weeks and so, when cathode and anode is consumed due to redox reaction, then the cells become unable to produce electricity.

Capacitors:

The capacitor is a device which is used to store electrostatic energy in the form of an electric field by storing charges inside it and thus creates a potential difference across its plates, similar to a small rechargeable battery. Today, many capacitors of several kinds are available in the market according to their use in the different areas of science such as a very small capacitor beads are used in resonance circuits while a large capacitor used in power factor correction, but they all do the same thing, they store charge. Charge storing property of a device measured in terms of capacitance, which is directly proportional to a dielectric constant of the material between the plates and the surface area of plates and inversely proportional to the plate separation.

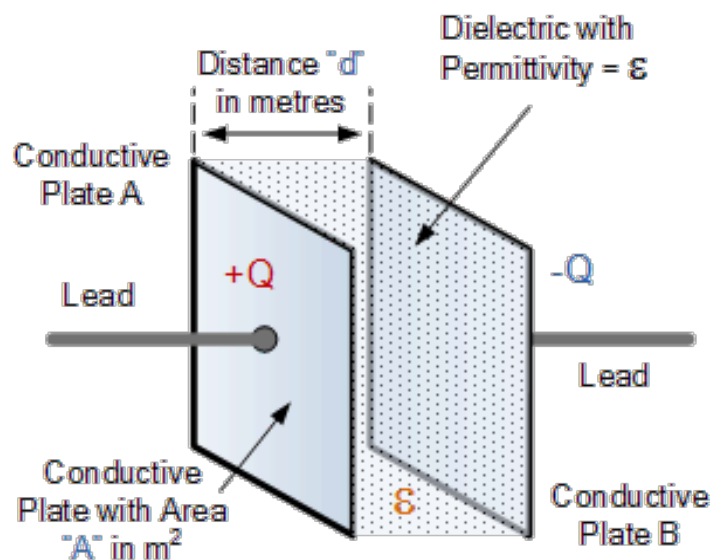


Fig. 1.2 A parallel plate Capacitor diagram^[4]

Compared to battery or fuel cells, capacitors always have a low energy density, but high power density and therefore can show fast charging & discharging but is not able to store a large amount of energy like batteries.

Supercapacitor:

A supercapacitor is a device that stores a large amount of charge via EDLC (Electric Double Layer Capacitance) and chemical redox

reactions phenomenon, and it is also called an ultracapacitor. Its capacitance is much higher in comparison to a simple electrolytic capacitor. It usually stores a Hundred times more energy than other ordinary capacitors. Due to its high power density capacitors can show fast charging and discharging that is far better than batteries and can tolerate longer life cycles than rechargeable batteries. A supercapacitor usually contains three essential parts 1) electrode, 2) electrolyte, and a separator, where electrode and its material has a significant role in the enhanced working of a supercapacitor. Therefore, it is a vital task to explore the electrode and its materials, which has excellent capacitive performance and has mega porosity. Their performance can be increased by modifying the structure of the material of electrode used. We can differentiate and compare battery, capacitor, and supercapacitor by looking at the following table 1(a).

Table 1(a). Approximate evolution between capacitor, battery and supercapacitor

Parameter	Capacitor	Battery	Supercapacitor
Charging time	Few microseconds to milliseconds	Hours	Milliseconds to minutes
Discharging time	Few microseconds to milliseconds	1-900 minutes	Milliseconds to days
Energy density (Wh/kg)	0.01-0.03	30-265	0.5-20
Power density (W/Kg)	>5000	100-300	5000-10000
Cycle life	>1 million	200-1000	Up to 1 million
Operating voltage(V)	6-800	1.2-4.2	1.0-4.5

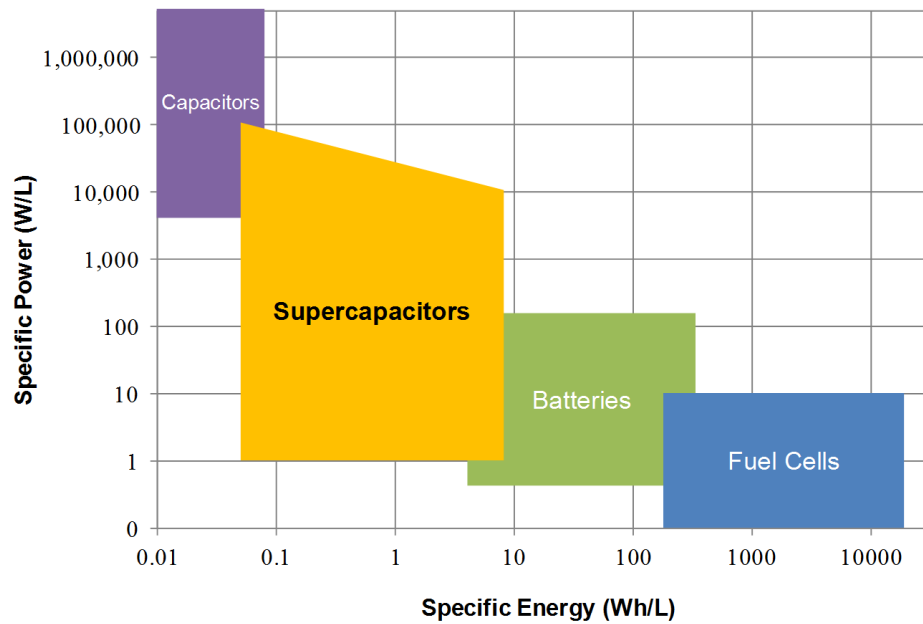


Fig.1.3 Ragone Plot^[6]

We have two different Energy storage mechanism in a supercapacitor that are given below as:-

- 1). EDLC (Electric double layer capacitance)
- 2). Pseudo capacitance

EDLC (Electric Double Layer Capacitance)

EDLCs are based on electrostatic charge diffusion with accumulation at the electrode-electrolyte interface. It has the following features which are listed below:-

- 1) No conventional dielectric but filled with electrolyte
- 2) Activated carbon as electrode provides large surface area
- 3) Long life cycle due to lack of any chemical reaction
- 4) Low energy storage due to lack of chemical reaction
- 5) Non-faradaic process

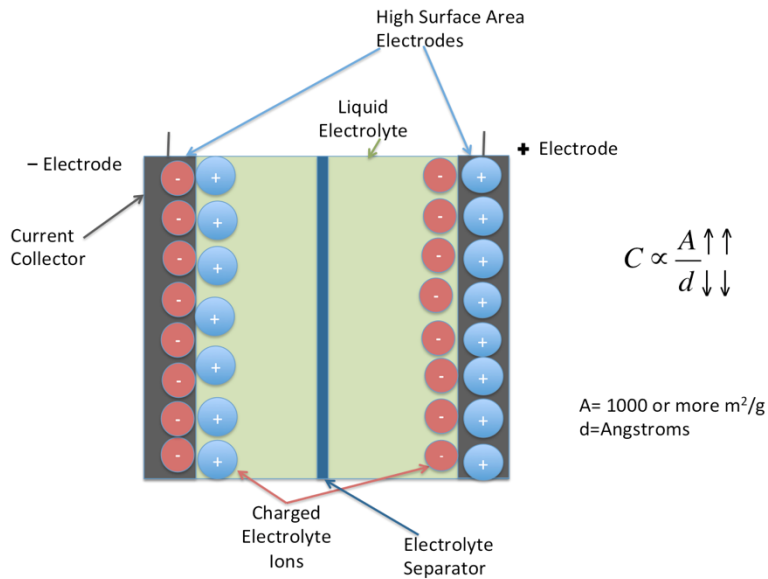


Fig. 1.4 Schematic diagram of EDLC.^[6]

Pseudo capacitance

1. It is a hybrid between battery and EDLC
2. It Stores charge via redox reactions and EDLC PROCESS
3. It High power density as well as high energy density in comparison of supercapacitor
4. It includes faradaic process.^[3-5]

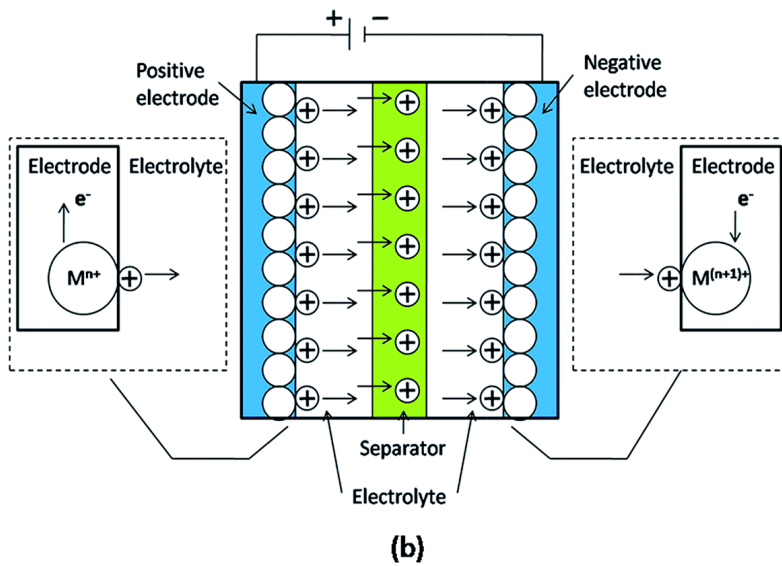


Fig. 1.5 Schematic diagram of pseudo capacitor.^[6]

Strategies to increase the capacitance of capacitor

Electrodes are the essential part of a supercapacitor, and their modification with different materials can enhance the charge holding ability of a supercapacitor. Thus we need a perfect strategy, and brilliant research work to build a successful energy storage driven economy. Materials with different conductivities and morphologies like nanorods, nanoflakes, nanosheets, nanowire, nanosphere, etc. can help us in the enhancement of energy storage and its electrochemical properties.

More importantly, all the properties as mentioned above with the charge storage enhancement for a supercapacitor is only possible by the use of nanotechnology. That's why nanotechnology is the emerging and fruitful branch of science.

1.1 Importance of Nanotechnology in the field of supercapacitors

The research in nanostructure and nanotechnology is becoming a growing field in the prominence of science and technology and material science. By the use of nanotechnology, we can create cheaper, smaller, economical devices for the betterment of the economy of the world. Nanoscience and technology are one of the most occult sciences of construction that can create nanostructure for the benefit of humanity. We also know that property of nanocrystal and the bulk of solids changes at the nanostructure level. Some of the features of nanostructure are discussed as:-

- it has high surface to volume ratio
- it can also provide tremendous surface area for supercapacitors
- it can also offer large specific heat
- it also possesses large thermal expansion
- it can also offer high catalytic activity
- it can also enhance self-diffusion
- it possess high magnetic susceptibility as well.

As the Surface to volume ratio is high, the surface area of the material will be increased by incorporating the nanomaterials, and the capacitance as well as its electrochemical properties will also be increased. Thus, nanotechnology can enable in the fabrication of electrode with higher surface area, porosity, varied morphology and dimension which will provide high charge storage and its efficient transport during the redox reaction. [4]

1.2 Hydrothermal synthesis

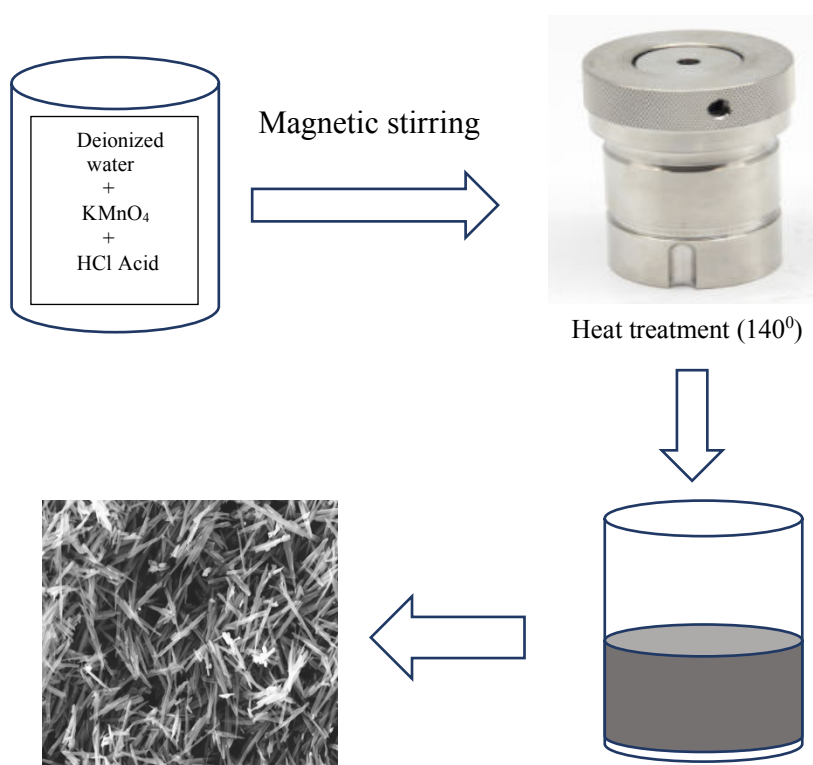


Fig. 1.6 Hydrothermal Synthesis Method

1.3 Motivation:

Transition metal oxide based electrodes for Supercapacitor applications

We are basically working on metal oxides, and here we have selected and synthesized the Manganese oxide (rods like morphology) because

- I. Transition metal oxide displayed pseudocapacitive behavior with high specific capacitance
- II. Transition metal oxide possess multiple oxidation states
- III. Multiple oxidation states increase the amount of redox reaction
- IV. Increased redox reaction helps in storing a large amount of charge hence energy density improved.

Different carbon materials show electrochemical double layered capacitance (EDLC) behaviour, while several transitions and noble metal oxides shows the pseudo capacitance behaviour. Among the different metal oxides that we have studied, Ruthenium oxide is supposed to be the promising pseudo capacitor material if used in acidic electrolyte but this much acidity can create environmental hazards, can also dissociate the metal ions during cycling process of capacitor and most importantly (RuO_2) is very costly which is not making it economically beneficial as well, therefore cannot be used for a big scale application such as in electric vehicles. The above-mentioned concerns motivate us for a search of an alternate material that has good and comparable electrochemical properties to Ruthenium oxide and will also be good for our environment and economy. Different metal oxides such as manganese oxide, Nickel oxide, Molybdenum oxide, Cobalt oxide and vanadium based oxides, etc., are being studied for their super-capacitive properties and Manganese oxide is found to be promising pseudo capacitor electrode material if we compared its specific capacitance, environmental compatibility, and cost effectiveness to other metal oxide but it has poor electrical conductivity and cyclic stability which still makes its performance limited for supercapacitance application. We

prepared manganese dioxide MnO_2 (alfa-form) by using the hydrothermal method of synthesis which is the economically good and also good for our environment. This method is used to prepare the nanostructure (nanorods) and we also prepared its hybrid by decorating Co_3O_4 nano-particles over MnO_2 to enhance its electrical conductivity and cyclic stability for energy storage applications^[5-6]

Objectives:

- To synthesize MnO_2 and its hybrid by decorating Co_3O_4 nano-particles over MnO_2 by simple and economical hydrothermal method.
- To characterize the material for Physico-Chemical properties.
- To study the supercapacitor applications of the MnO_2 and its hybrid.

CHAPTER-2

Material Synthesis & Characterization Techniques

2.1 Synthesis of α -MnO₂ Material

We have prepared our sample using hydrothermal technique where potassium permanganate was used as the precursor and after that below written steps were followed to complete material's synthesis.

1. 0.263 g of potassium permanganate (KMnO₄) was dissolved into 30 ml of double de-ionized water (18.2 MΩ cm) with stirring.
2. After 5 minutes of stirring, 1ml of conc. HCl (37%) was added.
3. Again it was left for 5 minutes for stirring, to get a complete homogenous solution.
4. Put the solution inside stainless steel autoclave of capacity 100ml and placed it inside muffle furnace at 140° C at the rate of 3° C/min for 16 hours.
5. The brown powder phase nanomaterial was collected by centrifugation process .
6. The resultant product was washed 3 to 4 times to remove impurities.
7. Sample was finally dried at 80°C for 24 hours .

2.2 Synthesis of the α -MnO₂/Co₃O₄ Material

Firstly, 0.263g of synthesized α -MnO₂ had been taken in a beaker and dissolved in 35ml of DI water. Then sonicated it for 30 minutes and after that kept it for stirring at least for 15 minutes. After doing this a well uniformly mixed α -MnO₂ solution was obtained in which we mixed 1mM(millimole) cobalt nitrate hexahydrate i.e. Co(NO₃)₂.6H₂O and again stirred it for 30 minutes. Now to have basic(PH ~11) solution ammonia was added in the solution in dropwise manner. Now the final solution was kept in furnace at 150°C for 12 hours using autoclave setup. After 12 hours a dark brownish precipitate was obtained which was

further kept for drying at 80°C for 12 hours. Finally hybrid of α -MnO₂/Co₃O₄ was obtained which was further characterised through different characterization techniques and electrochemical measurement were also carried out to have its specific capacitance.^[13-15]



(a) weighing balance



(b) Sonicator



(c) Autoclave.



(d) Furnace

Fig. 2.1 Lab instrument used for synthesis

2.3 Characterization technique

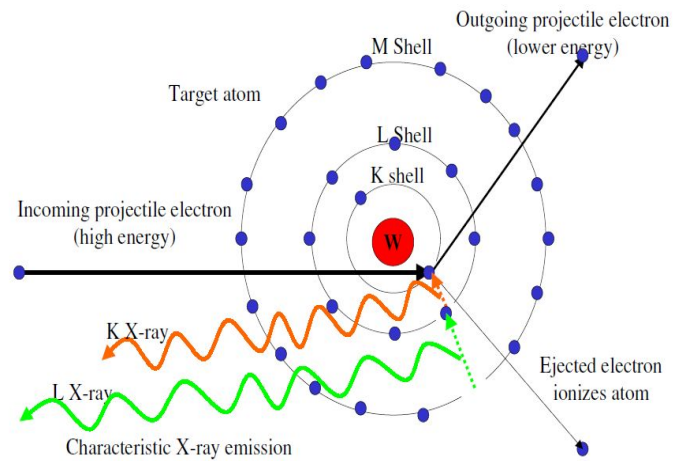
2.3.1 X-Ray diffraction (XRD)

(a) X-Ray introduction

X rays were first invented by Wilhelm Roentgen, a German professor of physics. According to him, electromagnetic radiation in a wavelength range (0.01 to 10 nanometre) commonly called X-rays. When high energy electron interacts in-elastically with an atom, the primary electron loses a detectable amount of energy(ΔE). This interaction will give rise to phonon scattering, plasmon scattering, characteristic X-ray, bremsstrahlung X-ray, Auger electron production,

etc. The schematics of characteristics of X-ray generation is shown in Fig. 2.2

Characteristic X-Ray Production



Continuous (Bremsstrahlung) X-Ray Production

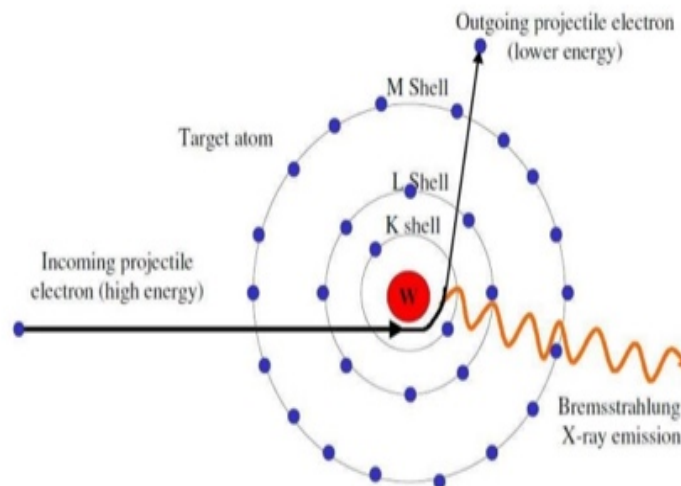


Fig. 2.2 Diagram showing the X-Ray production

X.R.D

For the characterization of crystalline material, one of the most powerful techniques that we used today is the X-ray diffraction (XRD) method. Not only this, it provides us the information regarding lattice and atomic parameters and also about atomic orientation as well.

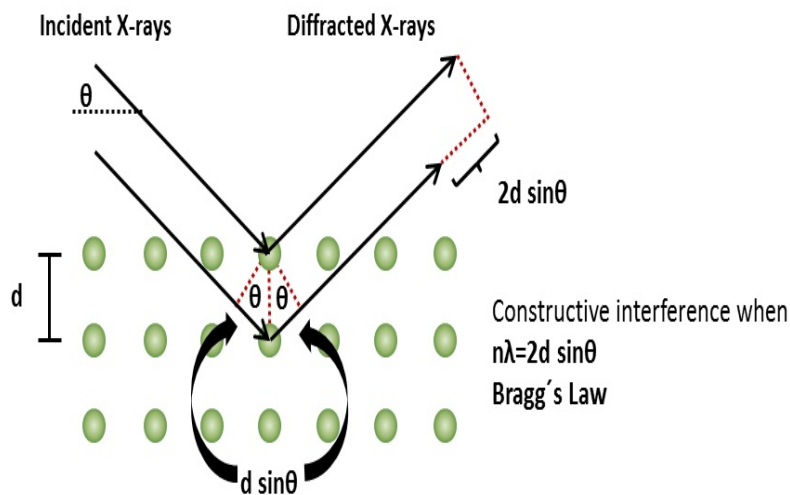


Fig. 2.3 Bragg's diffraction

The basic principle of X-Ray diffraction method is inference and diffraction of monochromatic X-rays beam which further scattered at different angles according to the orientation of crystal planes of atoms^[10-13]

The total path difference between two rays is:

$$= d \sin \theta + d \sin \theta$$

$$= 2d \sin \theta$$

When two separate waves arrive at a particular point with the same phase, then there is two possibility of constructive and destructive interference occurs where condition for undergo constructive interference is given as

$$2d\sin\theta = n\lambda$$

‘This is Bragg’s law of diffraction’.



Fig. 2.4 XRD Machine

2.3.2 Field Emission Scanning Electron Microscopy (FE-SEM)

A most powerful and versatile instrument that is available today to examine and analyse the microstructure morphology and chemical composition characterization is scanning electron microscope (SEM). A scanning electron microscope (SEM) is one of the types of microscopy where the surface of our sample is scanned through the electron beam and thus produces 3D images of our sample.

Working of SEM

As shown in Fig.2.5, the electron gun emits a electron beam that reaches to anode and is accelerated by the anode and then reaches to the focussing manganate after which it gets sharper and sharper. After this, when a beam reaches the surface of the sample, it produces, three kinds of electrons (1) secondary electrons (2) backscattered electrons (3) X- rays. These electrons are collected by the detectors and used to produce 2D images.

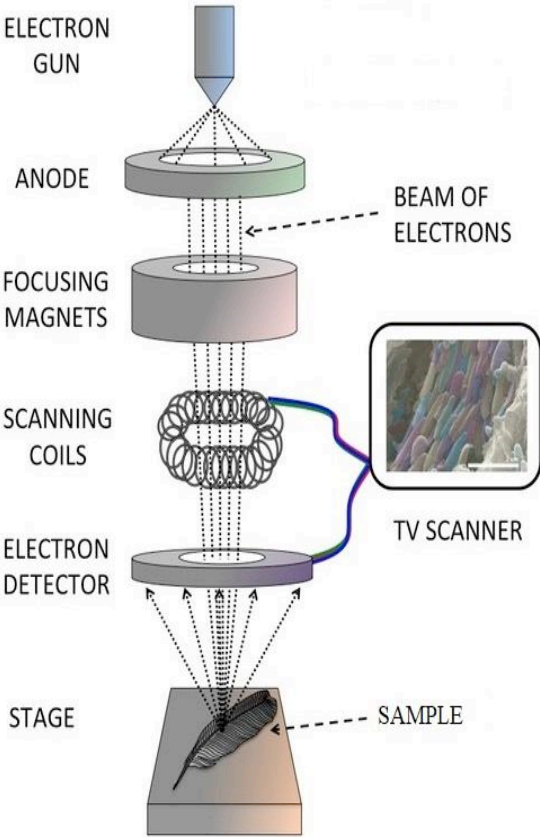


Fig. 2.5 Schematic working diagram of FE-SEM. [10]

Electron Beam and Specimen Interactions

Sources of Image Information

When the electron beam strikes the sample, both **photon** and **electron** signals are emitted.

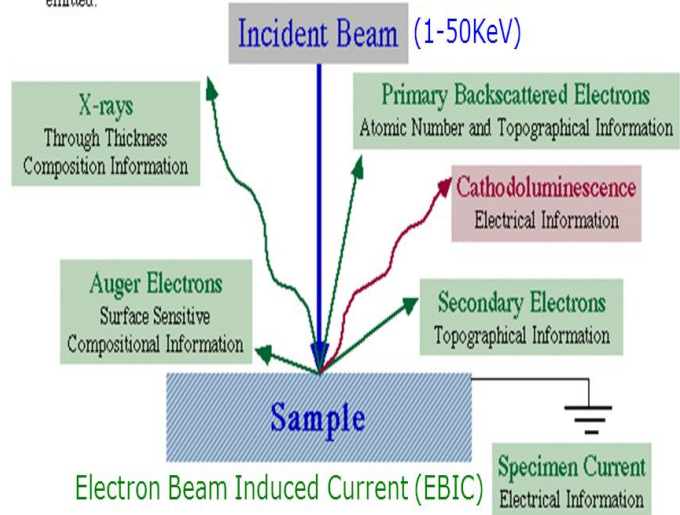


Fig. 2.6 Electron beam and sample interaction^[10]



Fig. 2.7 FE-SEM instrument setup at SIC, IIT Indore.

2.3.3 Transmission Electron Microscopy

A technique in which we used a beam of electrons and transmitted it through a specimen to form an image is called Transmission Electron Microscopy (TEM) microscopy. A high energy beam of electrons is incident and passed through a thin sample, and in results, there is an interaction between the electrons and the atoms happens and thus can be used to observe parameters such as particle size, morphology, crystal structure, dislocations, and grain boundaries. The TEM used the same basic principles as the optical microscope. It used an electron beam instead of a light beam. The schematic of the TEM is shown above in Fig. 2.8

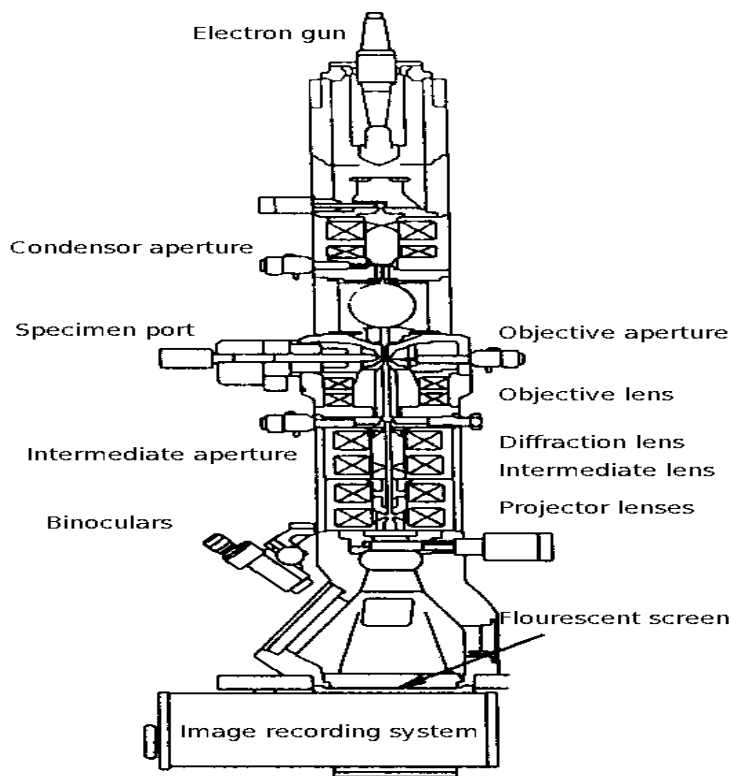


Fig. 2.8 Schematic diagram of TEM ^[12]

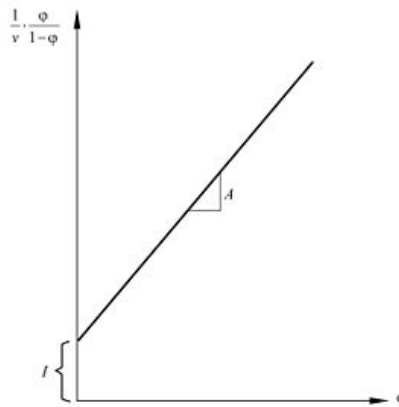
TEM usually have emission gun from which electrons are accelerated. TEM with >1000 kV acceleration potential has been developed for obtaining higher resolutions.

2.3.4 BET (Brunauer, Emmett and Teller).

Brunauer–Emmett–Teller (BET) theory explains and analyses the physical adsorption and desorption of gas molecules on a solid surface. Specific surface area is a property of solids which is considered as the total surface area of a material per unit of mass, solid or bulk volume or cross-sectional area. BET is used to estimate the surface area of nanostructures.

BET Equation

$$\frac{P}{V_{Total}(P_0 - P)} = \frac{1}{V_{Mono}C} + \frac{C - 1}{V_{Mono}C} \left(\frac{P}{P_0} \right)$$



V_{total} = Total volume of gas adsorbed at pressure P

V_{mono} = volume adsorbed by first layer

E_1 = Heat of adsorption of first layer

E_2 = Heat of liquefaction

P = Pressure when whole gas adsorbed

$$C = e^{\frac{(E_1 - E_2)}{RT}}$$

$$N_{Mono} = \frac{N_A V_{Mono}}{0.022414 \text{ m}^3 / \text{mol}}$$



Fig. 2.9 BET Facility at IIT Indore

2.3.5 UV-Visible Spectroscopy

It is a molecular spectroscopy in we usually study the interaction of Ultraviolet (UV)-Visible radiation with molecules and with the help of which we are able to find an energy band of a material. In this technique an ultraviolet light and a visible light is just passed through the material and after which the material absorbs some particular amount of wavelength which gives us the energy band gap with the help of tauc plot^[16]

The Wavelength of light absorbed will provide us the information on the energy bandgap, which is related to the functional group of the material. UV spectra of sample compounds are generally collected from 200-700 nm

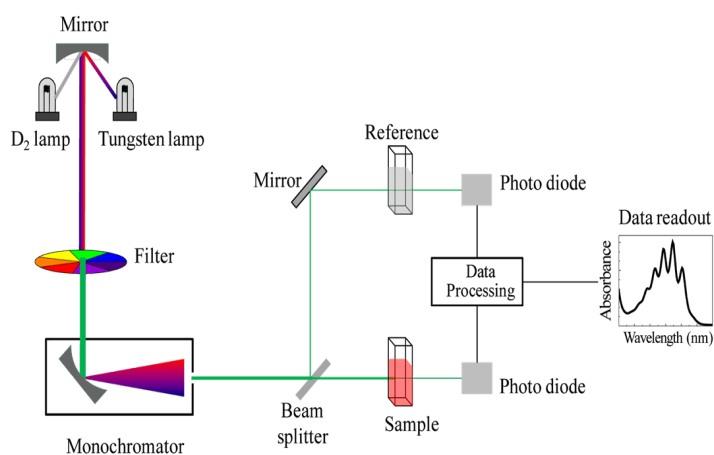


Fig. 2.10 Schematic for UV-Visible spectrometer^[16]

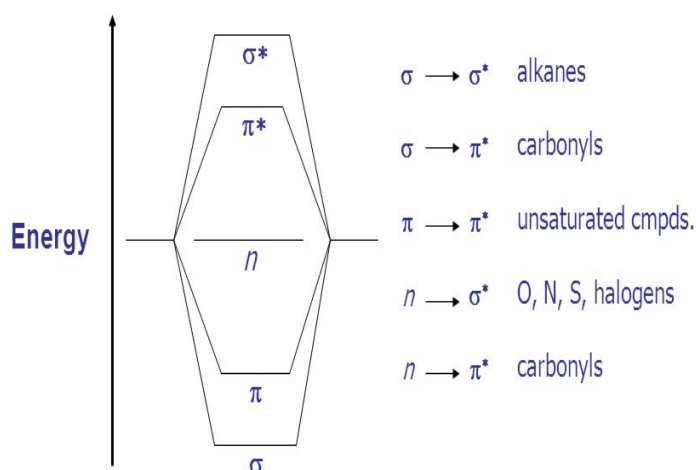


Fig. 2.11 Possible Transitions Organic Molecules^[18]

2.4 Cyclic Voltammetry

Cyclic voltammetry (CV) is a technique which is used to investigate the electrochemical behaviour of a system and was first reported by Randies^[14]. It provides us the considerable information on the redox processes, kinetics of electron-transfer reactions, and on coupled chemical reactions or adsorption process as well ^[15]

A CV is observed by applying a ramped linear potential (i.e., a potential that varies linearly with time) to the working electrode. This instrument consists of conventional three-electrode potentiostats connected to three electrodes (working, reference, and counter) immersed in a test electrolyte. The potentiostats applies and maintains the constant potential between the working and reference electrode while at the same time measuring the current between the counter and working electrode. A plotter is used to record the resulting CV as a graph of current versus potential.

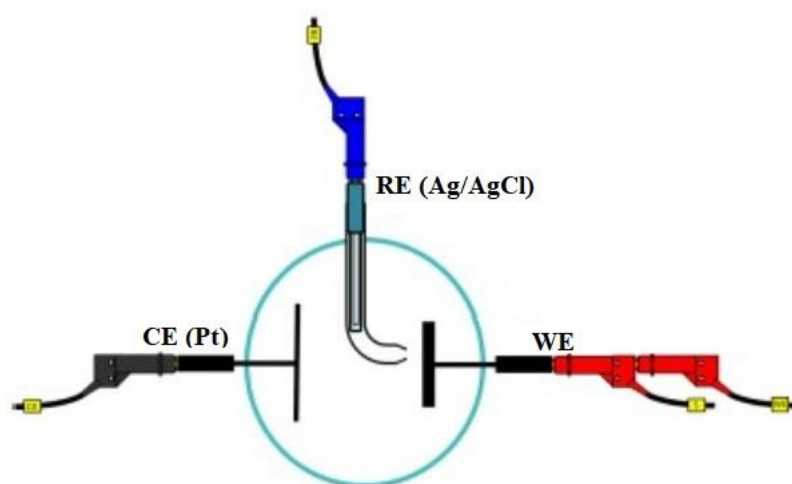


Fig. 2.12 Schematic view of 3 electrodes

Capacitance is given by charge divided by voltage, and it is termed to be specific when divided by mass. The charge can be written as a product of current and time. The Specific capacitance is given by the formula:

$$C = \frac{\int IdV}{mv\Delta V}$$

where, C = specific capacitance (F/g),

m = loaded mass,

ϑ = scan rate (V/s),

ΔV =potential window(in Volts),

$\int I.dV$ = area of the I-V graph plotted from the data received.

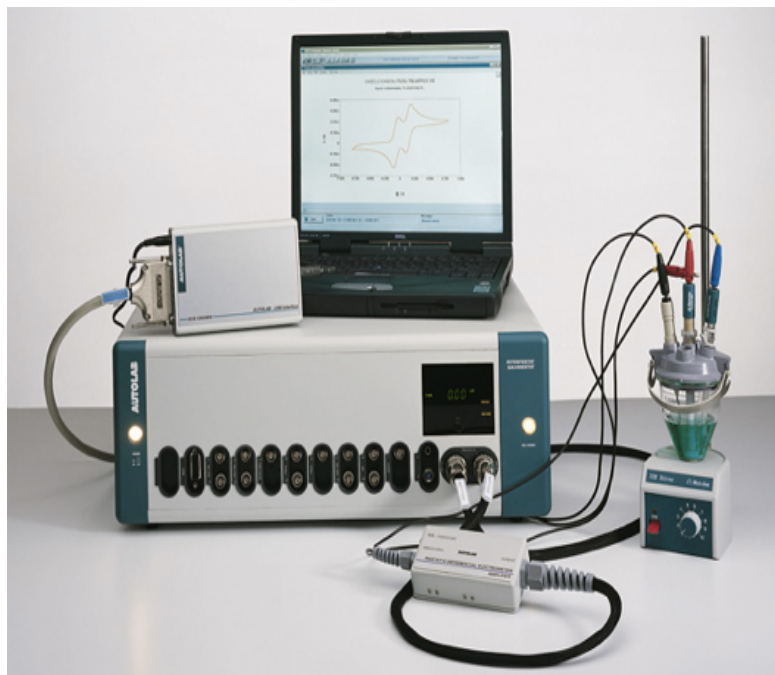


Fig. 2.13 Electrochemical Measurement Setup

2.5 Electrochemical Impedance Spectroscopy

Electrochemical Impedance Spectroscopy (EIS) not only measures the ability of a circuit element to resist the flow of electrical current but also measures our systems frequency response and its working progress with different frequencies. According to Ohm's law, resistance is defined in terms of the ratio between voltage E , and current I .

As we know The impedance (Z) is then represented as a complex number, $Z(\omega) = Z_0 \exp(j\Phi) = Z_0(\cos\Phi + j\sin\Phi)$

The expression of Z is composed of a real and an imaginary part. If the real part is plotted on X axis and the imaginary part on Y axis, we get a

‘Nyquist Plot’. In which the impedance can be represented as a vector of length $|Z|$.

Nyquist Plot has one major shortcoming, by looking at any data point on the plot, one cannot tell what frequency was used to record it.

2.6 Galvanostatic Charging Discharging

Galvanostatic charge-discharge (GCD) is a reliable method to evaluate performance, cycle-life, and the electrochemical capacitance of materials (EDLCs and batteries) under controlled current conditions. A repetitive loop of complete charging and discharging is called a cycle.^[30]

The value of specific capacitance (C) can be calculated with the help of GCD curve using the formula:

$$C = \frac{I\Delta t}{m\Delta V}$$

Where; C = the specific capacitance (F/g),

I = current (A), ΔV = the potential window

Δt = discharging time, m = deposited mass,

CHAPTER-3

RESULTS AND DISCUSSION

In this chapter, we discussed the results of α -MnO₂ and α -MnO₂/Co₃O₄ hybrid, which was characterized by X-ray diffraction (XRD), field emission scanning electron microscopy (FE-SEM), BET, UV-Visible spectroscopy. Electrochemical measurements of α -MnO₂ and α -MnO₂/Co₃O₄ hybrid were also carried out through cyclic voltammetry (CV), galvanostatic charging-discharging (GCD) and electrochemical impedance spectroscopy (EIS). These characterizations have helped in studying specific capacitance and material's behaviour response at different frequencies. The stability test for knowing the sustainability of the synthesized electrodes was carried through continuous cycles of GCD. The Electrolyte used for the electrochemical characterization was 1M KOH. The cyclic voltammetry was done upto 0.55V with different scan rate upto 90mV/s. Galvanostatic charging discharging measurement was also done at a voltage of 0.55V at different current density from 1, 2, 3, 5, 8 and 10 mA/cm². Stability test was done at a current of 8mA upto 2000 cycles. This chapter is divided into two parts: Part A α -MnO₂ and Part B Co₃O₄ decorated MnO₂. Part B by was carried out to increase the supercapacitive performance.

3.0 Physical Characterization

Part-A (Characterization of α -MnO₂ and Analysis)

A.1 X-Ray diffraction (XRD)

XRD pattern of the prepared material was investigated to know the crystal phase and crystallinity of the samples by using Bruker D2 Phaser XRD machine. Fig.3.1 shows the XRD pattern of α -MnO₂, which turn of phase-pure material with no impurities. All the XRD patterns peaks were indexed with tetragonal structure by comparing with [JCPDS 44-0141] card. Rietveld refinement was done from where we estimated

lattice parameters for α -MnO₂ are $a= 9.787(6)\text{\AA}$, $b= 9.786\text{\AA}$ and $c = 2.865(0)\text{\AA}$ and $\alpha=\beta=\gamma=90^\circ$.

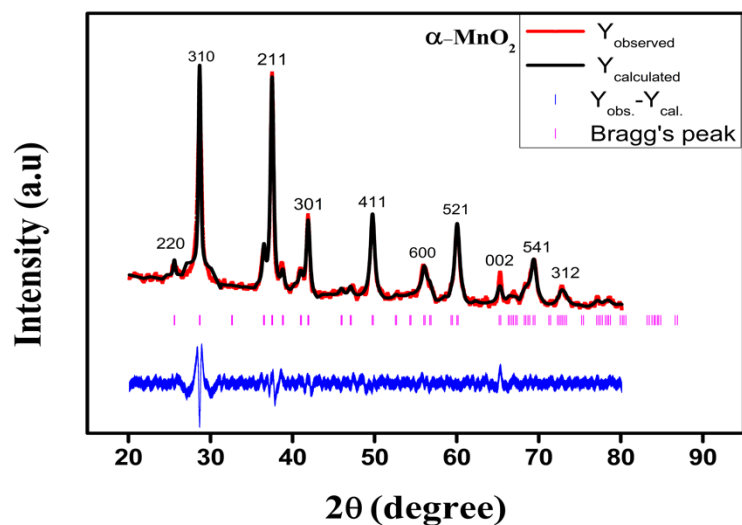


Fig. 3.1 XRD Pattern of α -MnO₂ nanostructure

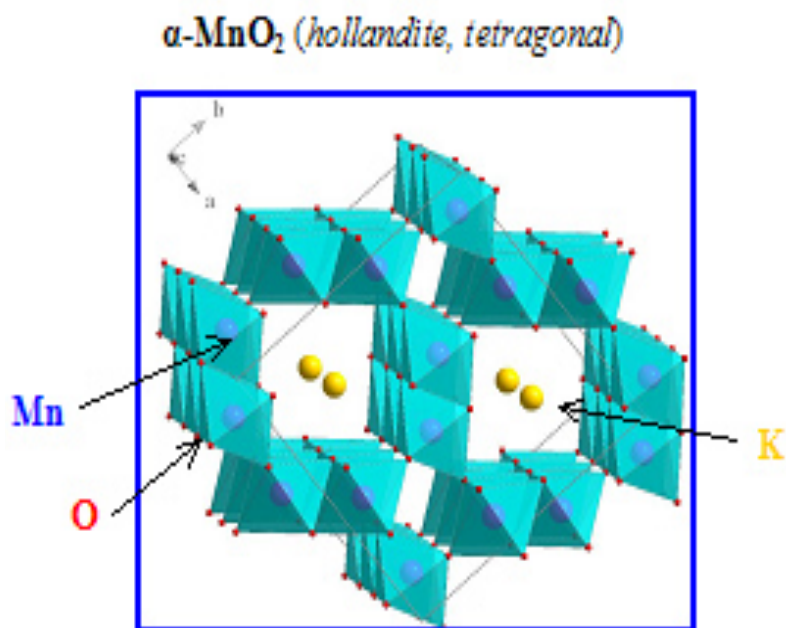


Fig 3.2. Geometrical structure of α - MnO₂ ^[22]

Fig.3.2 showed the structure of α -MnO₂ where the basic repeating unit of [MnO₆] octahedral can be seen that formed a (2 × 2) tunnel structure which is good for energy storage application.

A.2 Field Emission Scanning Electron Microscopy (FE-SEM)

Field emission scanning electron microscopy (FE-SEM) of α -MnO₂ nanostructure was carried out by using Supra 55 Zeiss model.

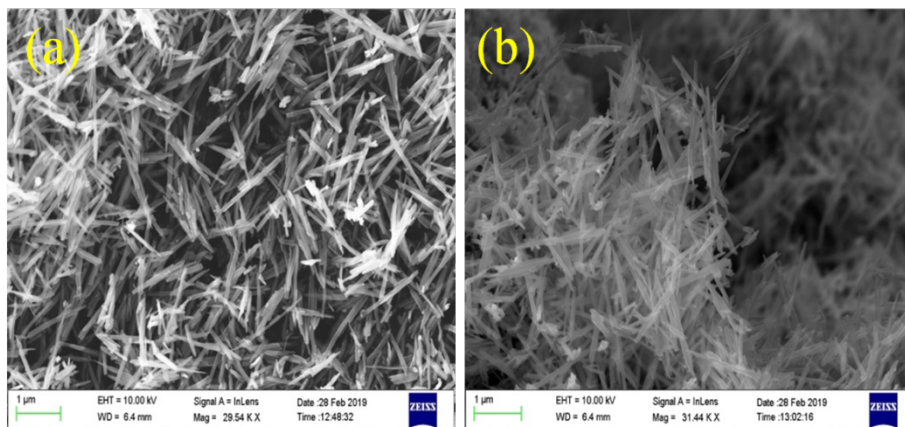


Fig. 3.3 FE-SEM micrographs of α -MnO₂ with magnification (a) 30 kX μ m and (b) 31.5kX

To know the morphology and porosity of the nanostructure, FESEM has been performed. The SEM micrograph, as shown in Fig. 3.3 showed the uniform distribution of nanorods of α -MnO₂. The nanorods like structure provided large surface area and porosity which is very credential for the supercapacitor properties. The large surface area provided a large platform for the interaction of electrolytic ions on the electrode whereas the porosity enhanced those interactions. The diameter of the nanorods was calculated as \sim 300nm.

A.3 Transmission Electron Microscopy (TEM)

Transmission electron microscopy (TEM) was also carried out and it was observed that α -MnO₂ sample was also composed of nanorods as it was confirmed by SEM. The TEM images are shown in Fig.3.4

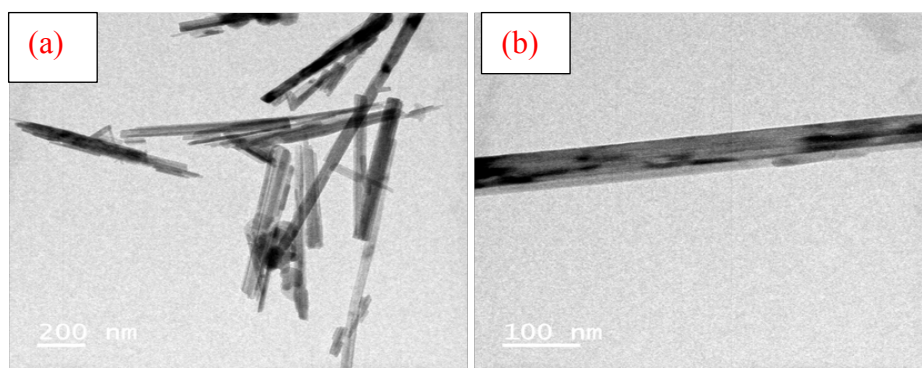


Fig 3.4 (a) and (b) TEM images of α - MnO_2 nanorods

A.4 UV-Visible Spectroscopy

The energy band gap of α - MnO_2 nanostructure was calculated using the UV-Vis absorption spectrum and it was recorded by using UV-2600 Shimadzu model. The sample shows a strong absorption peak (λ_{max}) at 483.20 nm in the UV region. This can be attributed to photo excitation of electron from valence band to conduction band. The optical energy band gap (E_g) was 1.63 eV calculated from tauc plot as shown in Fig. 3.5.

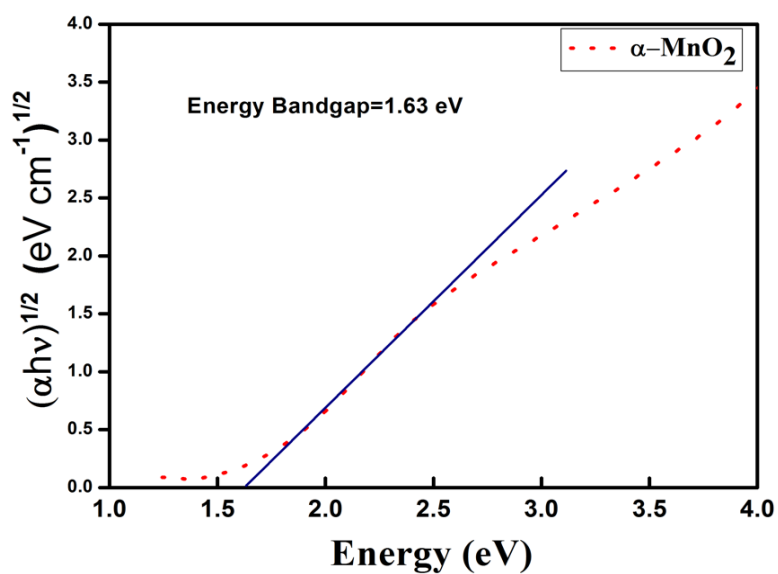


Fig. 3.5 Tauc Plot of α - MnO_2

A.5 Brunauer-Emmett-Teller (BET) surface area analysis

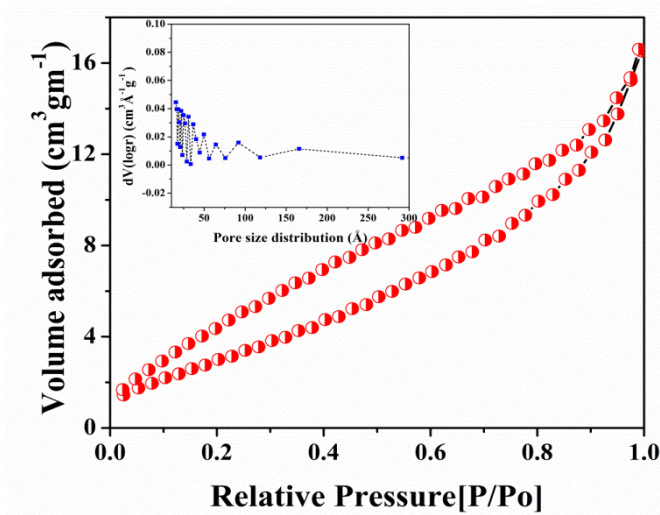


Fig. 3.6 Nitrogen adsorption-desorption isotherms and pore size distribution curves (inset) of α -MnO₂

The BET of the prepared sample α -MnO₂ has been done as shown in Fig 3.6. The specific surface area of α -MnO₂ was calculated to be 11 m²g⁻¹. The high surface area has an advantage for high electrochemical performance. The average pore diameter was calculated by BJH pore size distribution which was 3 nm approximately and it confirmed the mesoporous nature of the material. The mesoporous pore diameter is suitable for the mass transport and electrochemical activity. The large surface area of α -MnO₂ has mesoporous nature provided large charge storing capacity.

A.6 Electrochemical Measurement

To investigate the electrochemical redox behaviour of the prepared sample (CV) measurements were carried out as shown in Fig. 3.7. CV curve is shown at different scan rates of prepared sample using three electrode arrangement in 1M KOH electrolyte solution.

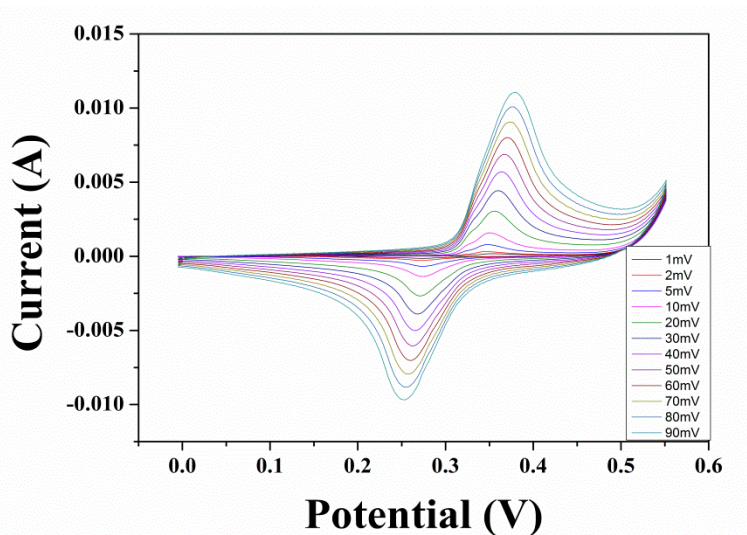


Fig. 3.7 CV curve of α - MnO_2 at different scan rates

CV was measured at different scan rates from 1 mV/s to 90 mV/s for a fixed potential window of 0.0V to 0.55 V as shown in Fig.3.7. The symmetrical oxidation peak and reduction peak indicated the existence of a highly reversible redox reaction. The CV curve area was changing when we increased the scan rate from (1 to 90 mV/s) that indicated the fast charging-discharging behaviour of material.

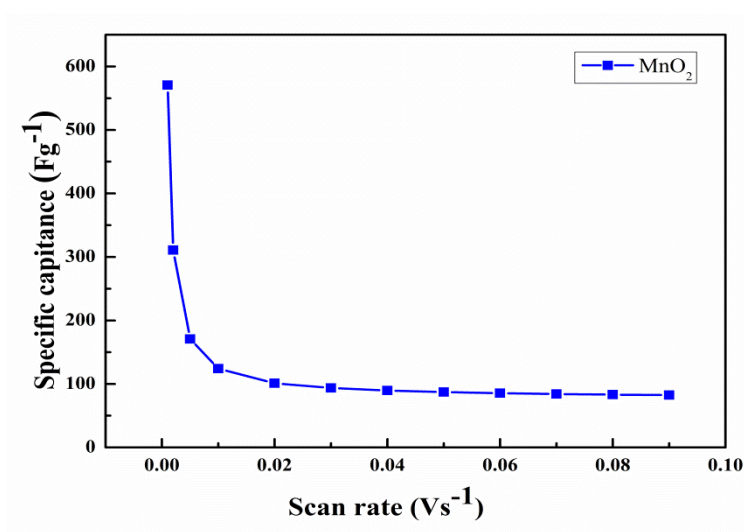


Fig.3.8 Variation of specific capacitance with scan rate.

Also Fig.3.8 was investigated where the highest capacitance of 570.4 F/g was obtained at 1 mV/s which decreased to 84 F/g at 90 mV/s. At lower scan rates the electrolyte ions get sufficient time to penetrate the pores of the material and thus have high specific capacitance while when the scan rate increased we noticed that capacitance decreased because pore penetration inside electrode becomes difficult due to high drifting of ions at high scan rate.

A.7 Electrochemical impedance spectroscopy

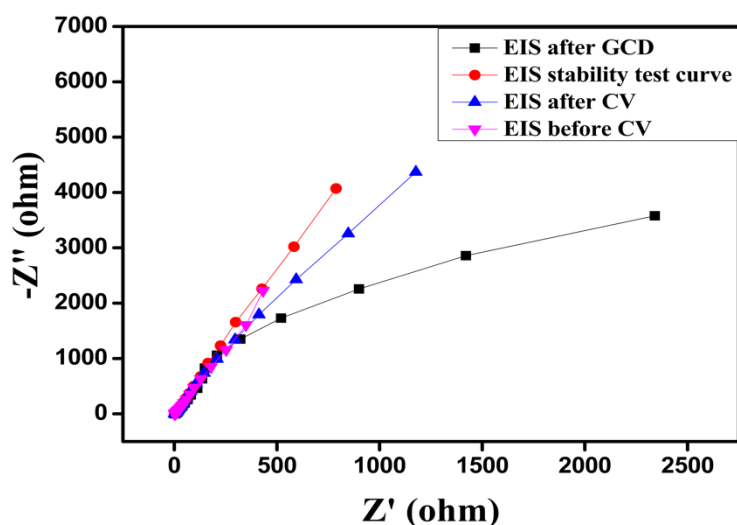


Fig. 3.9 EIS Spectroscopy of α - MnO_2

Fig. 3.9 shows EIS Spectroscopy of MnO_2 . The information achieved from figure 3.8 was that the synthesized electrode was acting as a capacitor because frequency dependent feature or impedance on a complex plane can be seen. It was clearly observed from the Fig. 3.9 that EIS done before CV has more capacitive behaviour and less resistive behaviour since it has more frequency dependence than the EIS done after CV. Therefore it was concluded that capacitive behaviour decreased and resistive behaviour increased after few cycle of charging and discharging. Similarly it was also concluded that the EIS done after GCD (Galvanostatic charging and Discharging) was showing a less capacitive behaviour and correspondingly resistive behaviour has increased.

A.8 Galvanostatic Charging-Discharging (GCD)

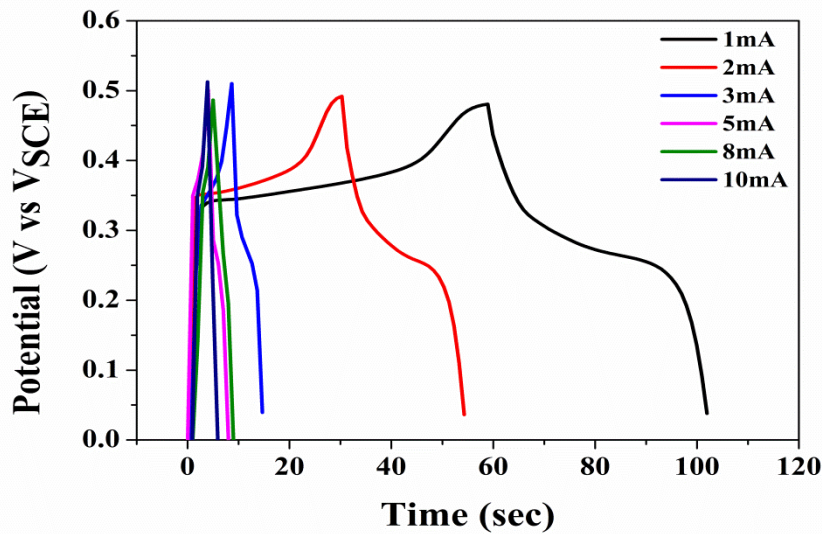


Fig 3.10 Galvanostatic charging/discharging plot of α -MnO₂

Galvanostatic charging discharging (GCD) measurements of α -MnO₂ electrode was carried out upto 0.5V at different values of current densities having rang from 1-10 mA/cm² as shown in Fig.3.10. GCD curves of α -MnO₂ electrode has varying plateau kind of structure *i.e.* it has two mixed state where one was regular triangular formation *i.e.* (EDLCs) effect and another has plateau formation *i.e.* (pseudo capacitor) effect with long charging/discharging time which can be understood as a pseudocapacitive or battery mimic behaviour of electrode. Highest capacitance of 570.4 F/g was reported at a current density of 1 mA/cm²

A plot that displayed the variation between capacitance and current density of electrode is shown in Fig.3.11, where electrode delivered a specific capacitance of 152.1F/g, 132.4F/g, 62F/g and 58 F/g, at different current densities upto 10 mA/cm² respectively. The gradual decrease with increase in current density can be analysed as incremental voltage drop which might be there because of the less active material was undergoing in redox process at higher current densities because of high drifting of ions in the solution.

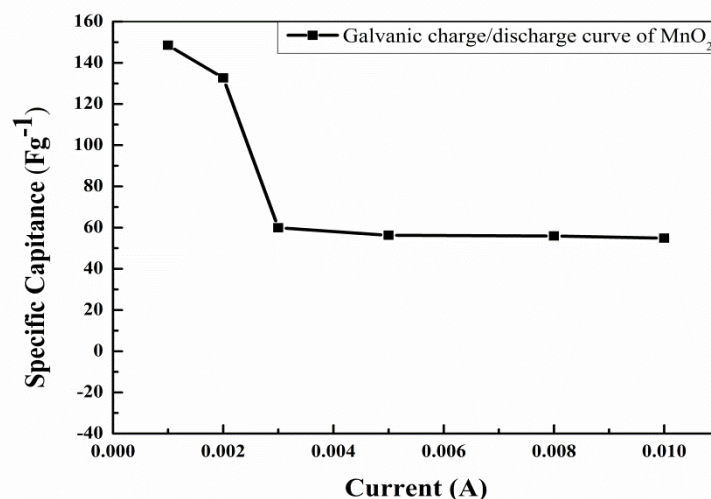


Fig. 3.11 Variation of specific capacitance with current density

A.9 Stability Test

To know the cyclic stability of α -MnO₂, capacitance retention was noted with the increasing number of cycle for the synthesized electrode and a graph was plotted from the repeated electrochemical measurement as shown in Fig.3.12. The measurement was done at a constant current density of 8 mA/cm² upto 2000 cycles. Specific capacitance of α -MnO₂ electrode remains about 96.5% after 2000 cycles, indicating an excellent behaviour of electrode material as well as long-term with the increasing current densities.

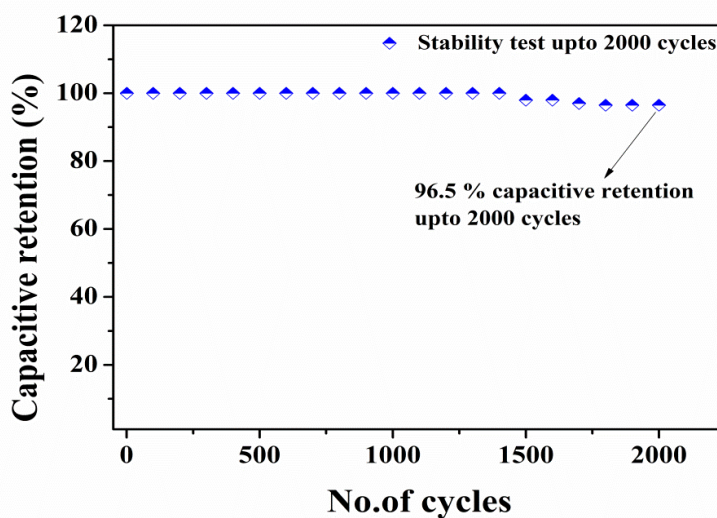


Fig. 3.12 Stability curve of MnO₂ nanostructure

Part- B α -MnO₂/Co₃O₄ Material

To increase the performance of the α -MnO₂ synthesized electrode, further it was hybridized with Co₃O₄, for attaining a synergistic effect of both α -MnO₂ and Co₃O₄. The hybrid nanostructure has been studied by various characterization techniques and electrochemical measurements were performed for the energy storage property.

Physical Characterization

B.1 XRD of α -MnO₂/Co₃O₄

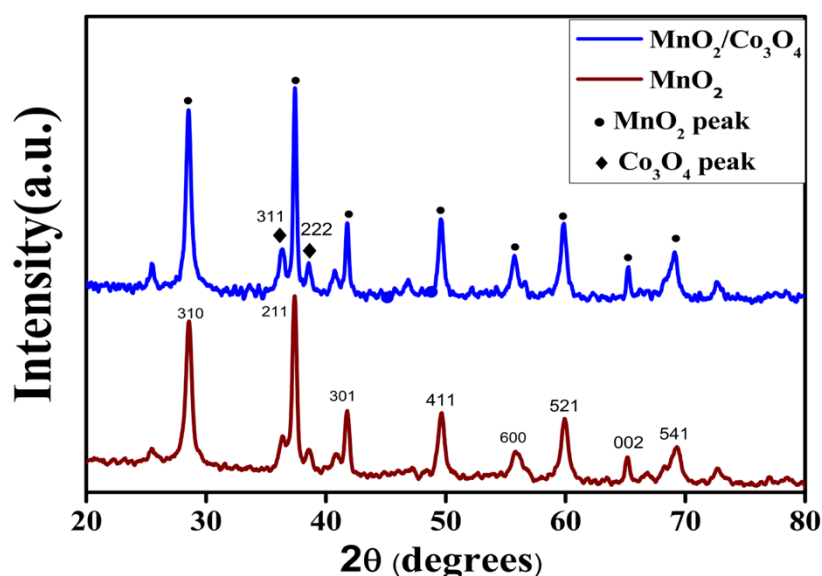


Fig.3.13 XRD Pattern of α -MnO₂ and α -MnO₂/Co₃O₄

XRD of α -MnO₂/Co₃O₄ is shown in Fig.3.13. It has two peaks of Co₃O₄ material that was decorated over the surface of α -MnO₂ nanorods at two angles 36.65° and 38.24° which were showing the (311) and (222) planes of Co₃O₄, respectively. Also, the low intensity of Co₃O₄ clearly indicated that the Co₃O₄ was just decorated over the surface of α -MnO₂ nanorods and has small nanoparticle size in comparison of α -MnO₂. It was clearly seen that phase pure α -MnO₂/Co₃O₄ hybrid nanomaterials has no impurity.

B.2 UV-visible spectroscopy

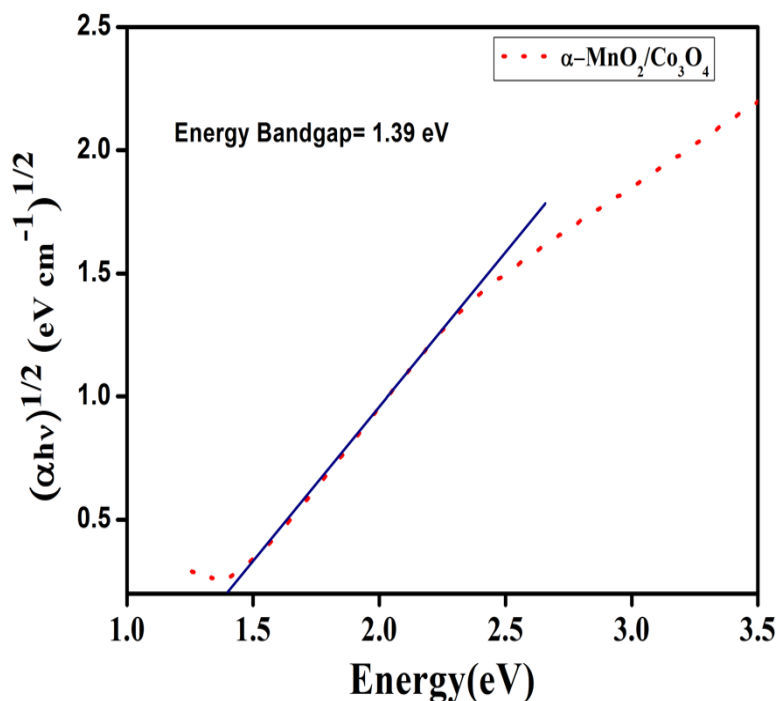


Fig.3.14 Tauc plot of $\alpha\text{-MnO}_2/\text{Co}_3\text{O}_4$

The energy band gap of $\alpha\text{-MnO}_2/\text{Co}_3\text{O}_4$ nanostructure was calculated using the UV-Visible absorption spectrum and it was recorded using UV-2600 Shimadzu model. The sample has a strong absorption peak (λ_{max}) at 539.20 nm in the visible region. This can be attributed to photo excitation of electron from valence band to conduction band. The optical energy band gap (E_g) was estimated 1.39 eV which was less than optical band gap of $\alpha\text{-MnO}_2$ that clearly indicated that the energy band gap of hybrid was decreased which made it more conductive than $\alpha\text{-MnO}_2$. Usually, more conductive material has more specific capacitance because electrons can be easily become free and thus available to increase specific capacitance of the material.

B.3 Field Emission Scanning Electron Microscopy

The SEM image of $\alpha\text{-MnO}_2/\text{Co}_3\text{O}_4$ is shown in Fig. 3.15. The uniform deposition of Co_3O_4 nanoparticles can be seen over the $\alpha\text{-MnO}_2$ nanorods. The size of the nanorods was found to be same as earlier.

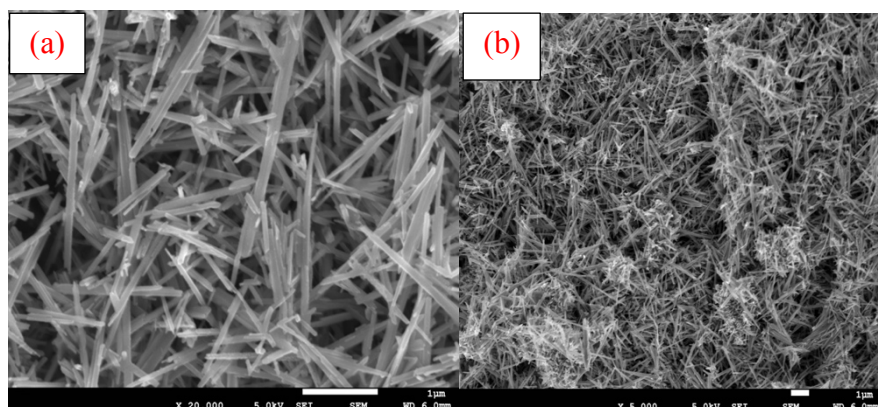


Fig. 3.15 FE-SEM Images of $\alpha\text{-MnO}_2/\text{Co}_3\text{O}_4$

B.4 Transmission Electron Microscopy (TEM)

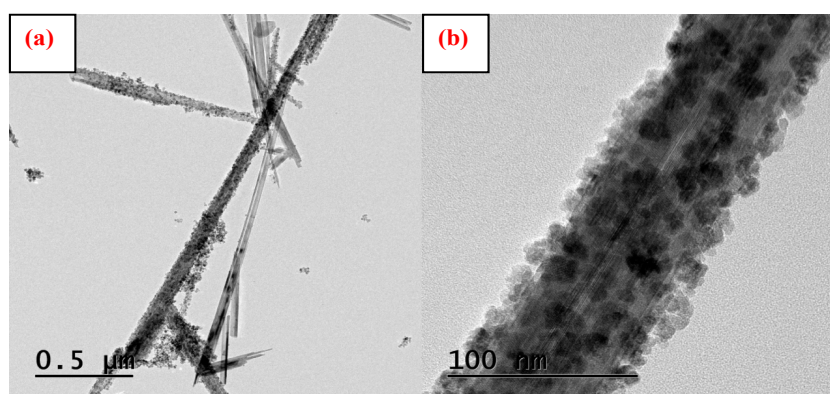


Fig 3.16 TEM images(a) and (b) of $\alpha\text{-MnO}_2/\text{Co}_3\text{O}_4$

When SEM of prepared sample was carried out, it was clearly seen in the Fig. 3.15(a) that $\alpha\text{-MnO}_2$ has the rod-like morphology but decoration of Co_3O_4 was not clearly visible in SEM images. Therefore, to further investigate the deposition of Co_3O_4 on $\alpha\text{-MnO}_2$ nanorods (TEM) was

carried out. TEM images of α -MnO₂/Co₃O₄ (hybrid) sample was shown in Fig.3.16 (b) which confirmed that Co₃O₄ nanoparticles were uniformly decorated over the α -MnO₂ nanorods.

B.5 Brunauer-Emmett-Teller (BET) surface area analysis

The BET of the prepared sample α -MnO₂/Co₃O₄ has been done as shown in Fig 3.17. The specific surface area of α -MnO₂ was calculated to be 33 m²g⁻¹ which is three times higher than MnO₂ (11 m²g⁻¹) as studied in earlier section. The high surface area has an advantage of high electrochemical performance. The average pore diameter was calculated by BJH pore size distribution which was 3 nm approximately and it confirmed the mesoporous nature of the material. The mesoporous pore diameter was suitable for the mass transport and electrochemical activity. The large surface area of α -MnO₂/Co₃O₄ has mesoporous nature can provide a large charge storing capacity.

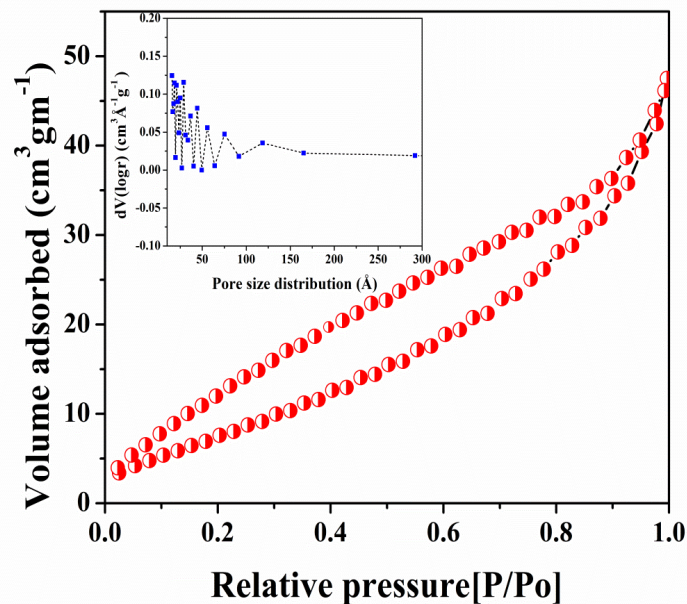


Fig 3.17: Nitrogen adsorption-desorption isotherms and pore size distribution curves (inset) of α -MnO₂/Co₃O₄ hybrid

B.6 Electrochemical Characterization α -MnO₂/Co₃O₄

B.6. 1 Cyclic Voltammetry

To investigate the electrochemical redox behaviour of the prepared sample α -MnO₂/Co₃O₄ hybrid CV measurements were carried out as shown in Fig. 3.18. CV curves are shown at different scan rates of prepared sample using three electrode arrangement in 1M KOH electrolyte solution. CV was measured at different scan rates from 1mV/s to 90 mV/s for a fixed potential window of 0.0V to 0.55 V as shown in Fig. 3.18. The symmetrical oxidation peak and reduction peak indicated the existence of a highly reversible redox reaction. The CV curve was not changing when we increased the scan rate from (1 to 90 mV/s) that indicates fast charging-discharging behaviour of material. We noticed that with the increasing scan rate its specific capacitance decreased as shown in Fig. 3.18. Highest specific capacitance with a value of 1802 F/g was reported at 1 mV/s for hybrid which decreases to 425 F/g at 90 mV/s. This high value of specific capacitance can be related to the hybrid nanorods which provided a large surface area with a highly porous structure for providing the fast diffusion.

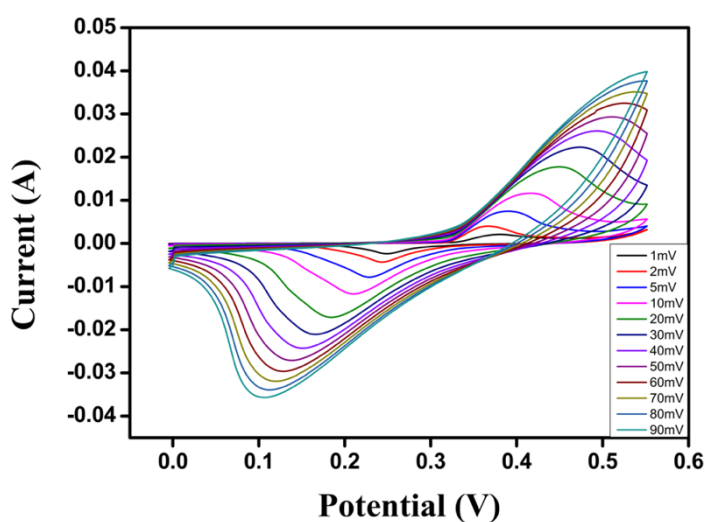


Fig. 3.18 CV of α -MnO₂/Co₃O₄ at different scan rate

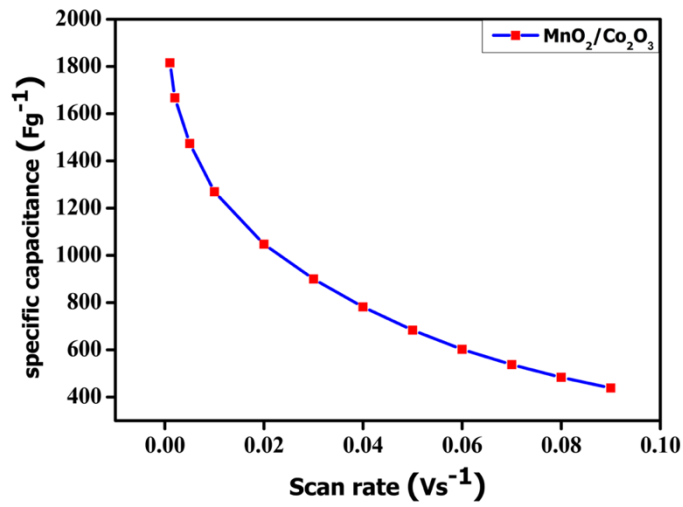


Fig. 3.19 Variation of specific capacitance with scan rate

B.7 Electrochemical impedance spectroscopy

The EIS measurement of α -MnO₂/Co₃O₄ has been performed as shown in Fig. 3.20 where we can see that all four graphs follows the same trend indicating the both capacitive and resistive behaviour of synthesized electrode.

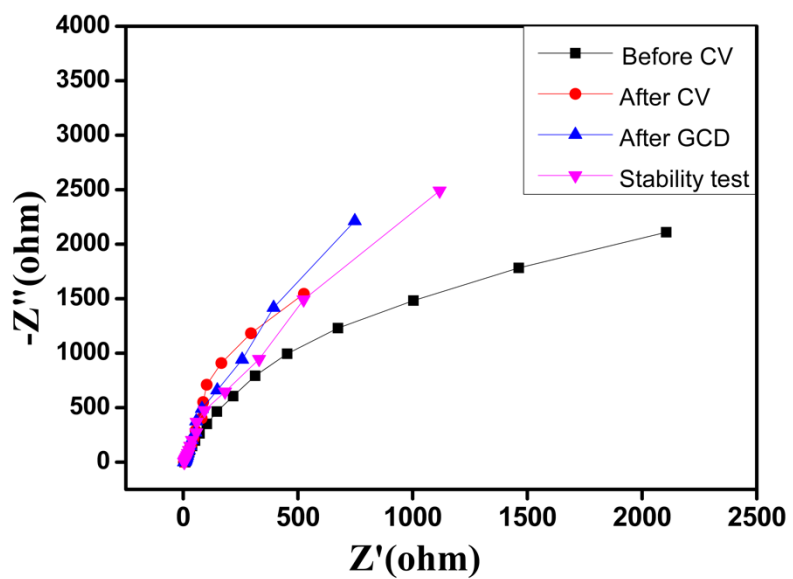


Fig. 3.20 EIS Spectroscopy of α -MnO₂/Co₃O₄

The Fig.3.20 is also showing that electrode was more frequency dependent on the large value of imaginary impedance showing more capacitive behaviour of the hybrid material. Hence capacitance of α -MnO₂/Co₃O₄ material was more than the previously formed α -MnO₂.

B.8 Galvanostatic Charging-Discharging

Galvanostatic charge-discharge (GCD) measurements of α -MnO₂/Co₃O₄ hybrid electrode was carried out within fixed potential window of 0 V-0.5 V at different values of current densities starting from 1, 2, 3, 5, 8 and 10 mA/cm² as shown in Fig. 3.21

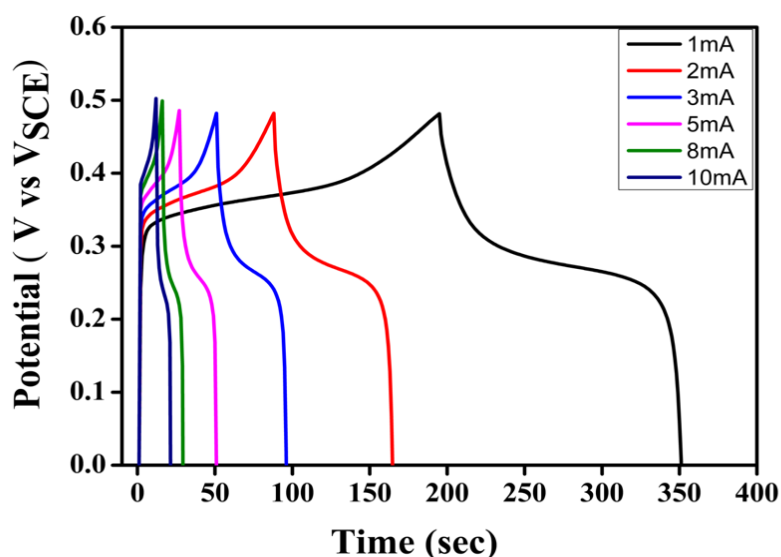


Fig 3.21 Galvanostatic charging/discharging plot

GCD curves of α -MnO₂/Co₃O₄ hybrid electrode is shown in Fig. 3.21. The formation of sloped plateau takes place in the α -MnO₂/Co₃O₄ hybrid nanomaterial *i.e.* we can easily observe the mixed state of a triangle indicated (EDLCs) effects and a plateau region indicated (pseudo capacitor) with a very long charging/discharging time period which can be understood as a pseudocapacitive or battery mimic like behaviour of electrode. Hybrid electrode has highest capacitance of 1802 Fg⁻¹ at a current density of 1 mA/cm². From GCD curve, the value of capacitance

came as high as 1809 F/g⁻¹ due to nanorods structure of electrode, which provided a good surface area for diffusion of charges on the of electrode surface, therefore providing path for very fast transport of electrons.

Fig.3.22 showed a the dependency of calculated specific capacitance on current density where one can easily see the trend of variation that capacitance was decreasing with the increase in current and also that electrode delivers a good specific capacitance of 700.1Fg⁻¹, 680.4Fg⁻¹, 590Fg⁻¹, 500Fg⁻¹, 430Fg⁻¹ and 390 Fg⁻¹, at current density of 1, 2, 3 ,5,8 and 10 mA/cm² respectively. The gradual decrease of specific capacitance with increase in current density can be related to incremental voltage drop across the device and because of this the less amount of diffusion was taking place inside or on the surface of electrode and thus capacitance decreased.

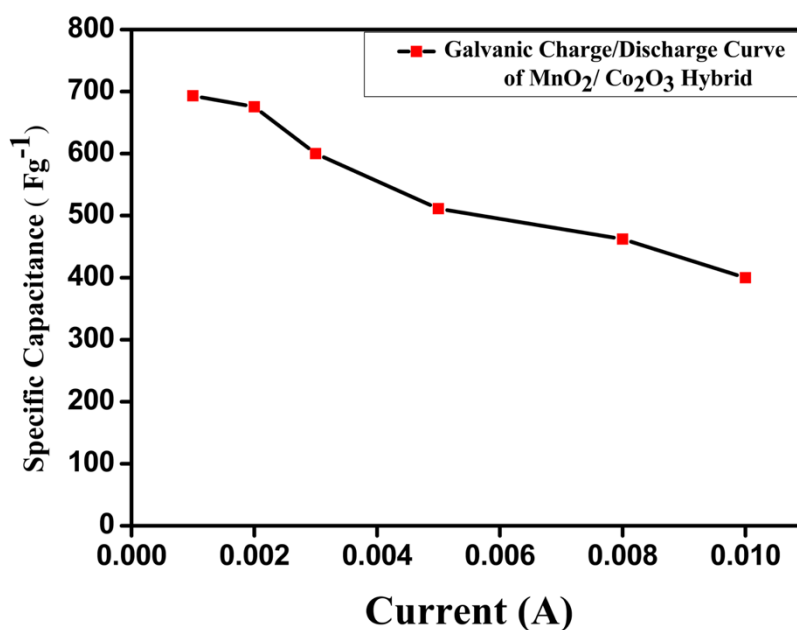


Fig. 3.22 Variation of specific capacitance with current densities

In summary, MnO₂ rods decorated with Co₃O₄ shows increase in supercapacitance behaviour. Hence good for the device fabrication.

Chapter-4

Summary and Conclusions and Future Scope

To conclude this thesis, Manganese dioxide (α -MnO₂) and its hybrid (α -MnO₂/Co₃O₄) was synthesized by hydrothermal technique. The synthesized α -MnO₂ and its hybrid (α -MnO₂/Co₃O₄) were confirmed by multiple physical characterization techniques. XRD confirmed the pure phase formation of α -MnO₂ and hybrid α -MnO₂/Co₃O₄. The formation of uniform nanorods like structure of α -MnO₂ was confirmed by SEM and the distribution of Co₃O₄ nanoparticles over α -MnO₂ nanorods were confirmed by TEM. The value of energy band gap was calculated as 1.63eV for α -MnO₂ and 1.39eV for its hybrid α -MnO₂/Co₃O₄ by using UV-Visible spectroscopy and tauc plot. BET surface area analyser showed the surface area of α -MnO₂/Co₃O₄ nanorods became nearly triple (11m²g⁻¹ to 33m²g⁻¹) which enhanced the charge storing capability of α -MnO₂/Co₃O₄.

Multiple electrochemical characterizations of prepared sample were carried out using three electrode systems. Cyclic voltammetry showed high specific capacitance of 570 Fg⁻¹ for α -MnO₂ and 1802.4. Fg⁻¹ for hybrid α -MnO₂/Co₃O₄ at Scan rate of 1 mVs⁻¹. GCD curve showed specific capacitance of 152.1Fg⁻¹and 700.1Fg⁻¹ at a current density of 1mA/cm² for α -MnO₂ and its hybrid α -MnO₂/Co₃O₄, respectively. Stability test for charging and discharging cycles showed good retention of 96.5% even after 2000 cycles.

Future Scope

It is highly desirable that we should have a balance point between performance and cost and α -MnO₂ is bridging that gap. Also, α -MnO₂ can be hybridized with other metal oxides (like Nickel, Tungsten, etc) to study electrochemical energy storage behaviour. Different morphologies

of α -MnO₂ with CNTs/graphene oxide can also be explored for enhancing super capacitance of the material. α -MnO₂ can be used to probe glucose level in blood in conjugation with other metal oxide/polymers.

In the coming future, there is a high probability that a full cell supercapacitor will have analogous energy density as lithium ion batteries would influence the market. That will bring an energy and storage revolution for the century with its outstanding performance and features in terms of energy storage.

References

1. Gidwani, Meet, Anand Bhagwani, and Nikhil Rohra. "Supercapacitors: the near Future of Batteries." *International Journal of Engineering Inventions* 4.5 (2014): 22-2.
2. Biswas, Md Multan, et al. "Towards implementation of smart grid: an updated review on electrical energy storage systems." *Smart Grid and Renewable Energy* 4.01 (2013): 122.
3. Shi, Fan, et al. "Metal oxide/hydroxide-based materials for super capacitors." *Rsc Advances* 4.79 (2014): 41910-41921.
4. Grove, T. T., M. F. Masters, and R. E. Miers. "Determining dielectric constants using a parallel plate capacitor." *American journal of physics* 73.1 (2005): 52-56.
5. Venkataraman, Anuradha. "Pseudocapacitors for energy storage." (2015).
6. Aslani, Marjan. "Electrochemical double layer capacitors (supercapacitors)." *Stanford University* (2012).
7. Duan, Xiaochuan, et al. "Controllable hydrothermal synthesis of manganese dioxide nanostructures: shape evolution, growth mechanism and electrochemical properties." *CrystEngComm* 14.12 (2012): 4196-4204.
8. Zhao, Xin, et al. "The role of nanomaterials in redox-based supercapacitors for next generation energy storage devices." *Nanoscale* 3.3 (2011): 839-855.
9. Weina, Xu, et al. "A novel β -MnO₂ micro/nanorod arrays directly grown on flexible carbon fiber fabric for high-performance enzymeless glucose sensing." *Electrochimica Acta* 225 (2017): 121-128.
10. Areef Billah, A. H. M. "Investigation of multiferroic and photocatalytic properties of Li doped BiFeO₃ nanoparticles prepared by ultrasonication." (2016).

11. Wu, Jianghong, et al. "Controllable hydrothermal synthesis of MnO₂ nanostructures." *Advances in Materials Physics and Chemistry* 3.03 (2013): 201.
12. Kong, Y. C., et al. "Ultraviolet-emitting ZnO nanowires synthesized by a physical vapor deposition approach." *Applied Physics Letters* 78.4 (2001): 407-409.
13. Sinha, Lichchhavi, et al. "Hybridization of Co₃O₄ and α -MnO₂ Nanostructures for High-Performance Nonenzymatic Glucose Sensing." *ACS Sustainable Chemistry & Engineering* 6.10 (2018): 13248-13261.
14. Bhojane, Prateek, et al. "Mesoporous layered hexagonal platelets of Co₃O₄ nanoparticles with (111) facets for battery applications: high performance and ultra-high rate capability." *Nanoscale* 10.4 (2018): 1779-1787.
15. Bhojane, Prateek, Somaditya Sen, and Parasharam M. Shirage. "Enhanced electrochemical performance of mesoporous NiCo₂O₄ as an excellent supercapacitive alternative energy storage material." *Applied Surface Science* 377 (2016): 376-384.
16. Sanchez-Hachair, Arnaud, and Annette Hofmann. "Hexavalent chromium quantification in solution: comparing direct UV-visible spectrometry with 1, 5-diphenylcarbazide colorimetry." *Comptes Rendus Chimie* 21.9 (2018): 890-896.
17. Jayalakshmi, Mandapati, and K. Balasubramanian. "Simple capacitors to supercapacitors-an overview." *Int. J. Electrochem. Sci* 3.11 (2008): 1196-1217.
18. Abraha, Ataklti, A. V. Gholap, and Abebe Belay. "Study self-association, optical transition properties and thermodynamic properties of neomycin sulfate using UV-Visible spectroscopy." *Int. J. Biophys* 6 (2016): 16-20.
19. K. Lota, A. Sierczynska, G. Lota, *International Journal of Electrochemistry*, (2011), 321473
20. M. D. Stoller, S. Park, Y. Zhu, J. And, R. S. Ruoff, *Nano Letters*, 8(10), (2008), 3948-3502
21. J.Randles, *Trans. Far. Soc.*, 44, (1948) 327.

22. Tompsett, David A., Stephen C. Parker, and M. Saiful Islam. "Surface properties of α -MnO₂: relevance to catalytic and supercapacitor behaviour." *Journal of Materials Chemistry* A2.37 (2014): 15509-15518.
23. Hibbert, D. Brynn. "Introduction to electrochemistry." *Introduction to electrochemistry*. Palgrave, London, 1993. 1-10.
24. S. Kannappan, K. Kaliyappan, R. Kumar, A. S. Pandian, H. Yang, Y. S. Lee, J. H. W. Lu, *Journal of Materials Chemistry A*, 2, (2012) 10652.
25. Zhang, Li Li, Rui Zhou, and X. S. Zhao. "Graphene-based materials as supercapacitor electrodes." *Journal of Materials Chemistry* 20.29 (2010): 5983-5992.
26. Downes, Andrew, and Alistair Elfick. "Raman spectroscopy and related techniques in biomedicine." *Sensors* 10.3 (2010): 1871-1889.
27. Nyström, Gustav, et al. "Self-assembled three-dimensional and compressible interdigitated thin-film supercapacitors and batteries." *Nature communications* 6 (2015): 7259.
28. Zhang, Li Li, Rui Zhou, and X. S. Zhao. "Graphene-based materials as supercapacitor electrodes." *Journal of Materials Chemistry* 20.29 (2010): 5983-5992.
29. E. Gileadi, E. K. Eisner, J. Penciner, "Interfacial Chemistry: An Experimental Approach" (Addison-Wesley Eds), 1975
30. Bard, Allen J., et al. *Electrochemical methods: fundamentals and applications*. Vol. 2. New York: Wiley, 1980.